RSC Advances

ROYAL SOCIETY OF CHEMISTRY

www.rsc.org/advances

Journal Name

ARTICLE

Highly tough and puncture resistant hydrogels driven by macromolecular microspheres

Received 00th January 20xx,
Accepted 00th January 20xx

DOI: 10.1039/x0xx00000x

www.rsc.org/

Xiu Yan Ren, Zhe Yu, Baijun Liu, Xue Jiao Liu, Ya Jun Wang, Qiang Su, Guang Hui Gao *

Traditional hydrogels with poor mechanical properties have the largest barrier for extensive practical applications, such as artificial tendon, cartilage, skins and so on. In this work, a novel design strategy is proposed and demonstrated to improve the mechanical behavior of hydrogels by introducing ductile macromolecular microspheres (MMs) as crosslinking centers. Firstly, the macromolecular microspheres are synthesized using butyl acrylate (BA) as a main component and dicyclopentyl acrylate (DCPA) as an intermolecular crosslinker by a conventional emulsion polymerization method. Then acrylamide (AM) and hexadecyl methacrylate (HMA) are crosslinked by MMs in water to form MMs crosslinked poly(acrylamide-co-hexadecyl methacrylate) (P(AM/HMA)-MMs) hydrogels. From the tensile measurement, the P(AM/HMA)-MMs hydrogels exhibit dramatic enhancement of fracture stress σ_f (0.555MPa) and fracture strain ε_f (5533%) comparing to original P(AM/HMA) hydrogels. Moreover, the P(AM/HMA)-MMs hydrogels also reveal the excellent puncture resistant property. Based on traditional mechanisms of rubber-toughened plastics, it is clear that MMs can not only prevent the further development of cracks but also be stretched to deform and absorb a large amount of energy. It is envisioned that the novel strategy, inspired by toughening mechanism, will be an effective approach to enhance the mechanical property and broaden the application scale for hydrogels.

Introduction

Hydrogels with a three-dimensional network structure could hold a large amount of water and simultaneously keep their shape. They had drawn a considerable attention due to their wide applications, such as tissue scaffolds[1, 2], drug delivery vehicles[3-5], cell supports[6] etc. However, the conventional hydrogels showed a poor mechanical property because of the heterogeneous network structure, limiting the application range of tissue engineering, such as artificial cartilage, tendon, muscle and blood vessel[7]. Therefore, a large number of investigations had been focused on developing new mechanisms for toughening hydrogels, including double network hydrogels[8], slide-ring hydrogels[9], nanocomposite hydrogels[10-13], tetra-PEG hydrogels[14], clay composite hydrogels[15], macromolecular microsphere composite hydrogels [16-18] and hydrophobic association hydrogels[19-22].

The hydrophobic association hydrogels were composed of hydrophilic components and hydrophobic segments. The hydrophobic chains could be assembled into micelle-like aggregates by molecular entanglement as physical cross-linking points in hydrogels. When the hydrogels were loaded and deformed, the curl hydrophobic chains could slide and be stretched so that large amounts of energy would be dissipated. Liu et al. had reported a method of obtaining hydrophobic association hydrogels with a new hydrophobic molecule of octylphenol pohyixyethylene ether acrylate[21-22]. Introducing the hydrophobic monomers into hydrogels seemed to be a feasible way to increase the mechanical strength. However, the simple physical interaction force between the hydrophobic chains was weak so that the tensile strength was not enough high comparing to that of hydrogels with chemical bonds.

Macromolecular microspheres (MMs) were usually environmentally sensitive and mainly used in a drug delivery system. However, it was difficult to form bulk hydrogels. Even if there were some hydrogels formed by macromolecular microspheres, the mechanical property of hydrogels was poor. Subsequently, microspheres had been introduced to bulk hydrogels to improve their strength[23-26]. For example, peroxidized microspheres with a diameter 100 nm were acted as both initiators and cross-linkers, grafting poly(acrylic acid) chains onto the surface of microspheres. As a result, hydrogels exhibited a good compressive performance, but the tensile and tearing properties, which truly reflected resistance against crack propagation, had not been reported[17].

Herein, we reported a novel method of MMs crosslinked hydrogels with highly tough and puncture resistant properties. The MMs were prepared of butyl acrylate as a main component and dicyclopentyl acrylate as an intermolecular crosslinker by a one-

[a] Engineering Research Center of Synthetic Resin and Special Fiber, Ministry of Education, Changchun University of Technology, Changchun, P. R. China
[b] School of Chemistry and Life Science, and Advanced Institute of Materials Science, Changchun University of Technology, Changchun, P. R. China
[c] Corresponding author: Guang Hui GAO, Tel: +81-431-85717352, Fax: +81-431-85716465, E-mail: ghgao@ccut.edu.cn
† Footnotes relating to the title and/or authors should appear here.
Electronic Supplementary Information (ESI) available: [details of any supplementary information available should be included here]. See DOI: 10.1039/x0xx00000x

step emulsion polymerization method[27, 28]. Subsequently, the highly tough hydrogels were prepared by using acrylamide (AM) and hexadecyl methacrylate (HMA) as main chains and MMs as a chemical crosslinker. Inspired by traditional mechanisms of rubber-toughened plastics[29, 30], MMs would not only prevent the crack development, but also stretch after the deformation of substrates to enhance the break elongation. It was envisioned that MMs crosslinked hydrogels could exhibit high tensile strength and long elongation at break. The structure and formation mechanism for MMs crosslinked P(AM/HMA) hydrogels were proposed in Fig. 1. The novel strategy would open a new avenue for toughening hydrogels and be an effective approach to broaden the biomedical applications of hydrogels.

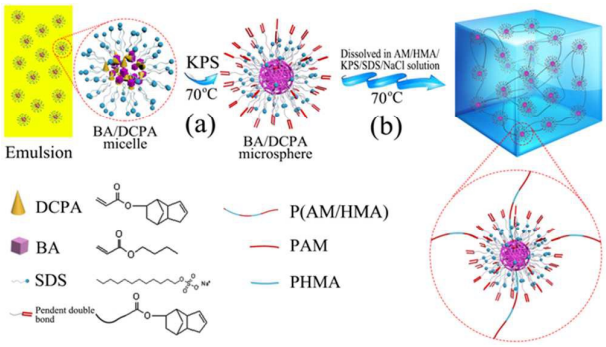

Fig. 1 Structure and formation mechanism of MMs crosslinked P(AM/HMA) hydrogels.

Experimental Part

Materials

Acrylamide (AM, 99.0%), 4-arm poly(ethylene glycol) acrylate (4-arm PEG-AA, molecular weight 2000), sodium dodecysulfate (SDS, ≥97%), potassium persulfate (KPS, 99.5%), sodium chloride (NaCl, 99.5%), butyl acrylate (BA), dicyclopentyl acrylate (DCPA, 99.5%), sodium carbonate (Na_2CO_3, >99.0%) were supplied by Aladdin (Shanghai, China), hexadecyl methacrylate (HMA, 95%) was supplied by Zhejiang Kangde New Materials Co., Ltd, China. BA was distilled under reduce pressure, and was stored at −18 °C. Deionized water was used in the experiment.

Preparation of MMs

A series of experiments were carried out in order to obtain different particle size of MMs. The following variables were investigated: SDS molar percentage was changed in the range of 0.55mol% to 2.75mol% for BA, Na2CO3 molar percentage was investigated in the range of 0.6mol% to 3.0mol% for BA, DCPA and KPS molar percentage were also for BA. The fundamental recipe used to prepare MMs latexes was listed in Table1.

Deionized water, SDS, Na_2CO_3 were charged to a three-necked boiling flask and dissolved. SDS and Na_2CO_3 were used as emulsifier and electrolyte, respectively. Then, monomer (BA) and crosslinking agent (DCPA) were added to the reactor and kept at 70 °C, and nitrogen gas was flushed to remove the oxygen (about 30 min). Initiator (KPS) was charged into the reactor after dissolving in some deionized water. The rate of nitrogen bubbling was decreased to minimize evaporation. The reaction time zero was taken at this point .The reaction time was set up to 120 min in order to obtain a high conversion for the experiments. Finally, we obtained MMs latexes.

Table1. Recipe for preparation of MMs latexes

MMs	BA/water (wt%)	DCPA (mol%)	SDS (mol%)	KPS (mol%)	Na_2CO_3 (mol%)
a	40/60	2	2.75	0.0064	0.6
b	40/60	2	2.20	0.0064	1.2
c	40/60	2	1.65	0.0064	1.8
d	40/60	2	1.10	0.0064	2.4
e	40/60	2	0.55	0.0064	3.0

Preparation of Hydrogels

Preparation of PAM-MMs hydrogels

NaCl and SDS was dissolved at room temperature in deionized water by constant stirring to prepare 5% SDS/ 0.4 M NaCl aqueous solution. After the solution changed transparent, the MMs emulsion was added into the solution and stirred for 2 h to make MMs disperse completely. KPS and AM were added into the beaker and stirred for 10min, KPS molar percentage was 0.01mol% for AM. Then, the solution in the beaker was poured into the mold consisting of two parallel glass plates and 3mm silicone spacer and then kept at 70 °C for 3h to obtain PAM-MMs hydrogels.

Preparation of P (AM/HMA) hydrogels

NaCl and SDS was dissolved at room temperature in deionized water by constant stirring to prepare 5% SDS/ 0.4 M NaCl aqueous solution. After the solution changed transparent, HMA was added into the solution and stirred for 2 h to make HMA disperse completely. KPS and AM were added into the beaker and stirred for 10min, KPS molar percentage was 0.01mol% for AM. Then, the solution in the beaker was poured into the mold consisting of two parallel glass plates and 3mm silicone spacer and then kept at 70 °C for 3h to obtain P(AM/HMA) hydrogels.

Preparation of P (AM/ HMA/PEGAA) hydrogels

NaCl and SDS was dissolved at room temperature in deionized water by constant stirring to prepare 5% SDS/ 0.4 M NaCl aqueous solution. After the solution changed transparent, HMA was added into the solution and stirred for 2 h to make HMA disperse completely. AM, 4-arm PEGAA and KPS were added into the beaker and stirred for 10min. Mass fractions of AM in an aqueous medium was 25%, KPS molar percentage was 0.01mol% for AM, 4-arm PEGAA molar percentage was 0.05mol% for AM. Then, the solution in the beaker was poured into the mold consisting of two parallel glass plates and 3mm silicone spacer and then kept at 70 °C for 3h to obtain P (AM/ HMA/PEGAA) hydrogels.

Preparation of P (AM/HMA)-MMs hydrogels

NaCl and SDS were dissolved at room temperature in deionized water to prepare 5% SDS/ 0.4 M NaCl aqueous solution. After the solution changed transparent, the HMA and MMs emulsion (the mass content of MMs in adding monomers was 0wt%, 0.5 wt%, 1 wt% and 1.5 wt%) were added into the solution and stirred for 4 h to make HMA and MMs disperse

completely. KPS and AM were added into the beaker and stirred for 10min, KPS molar percentage was 0.01mol% for AM. Then, the solution in the beaker was poured into the mold consisting of two parallel glass plates and 3mm silicone spacer and then kept at 70 °C for 3h to obtain P(AM/HMA)-MMs hydrogels. The formulations of P(AM/HMA)-MMs hydrogels were denoted as P(AMx/HMAy)-MMs(j,k). Here, x was mass fractions of AM in an aqueous medium, y was mole fractions of HMA for AM, j was mass fractions of MMs for AM and HMA, and k was the particle size of MMs, respectively. The detail compositions of hydrogels were shown in Table 2.

Table 2. The components of MMs crosslinked hydrogels

$P(AM_x/HMA_y)$-$MMs_{(j,k)}$	AM(wt%)	HMA(mol%)	MMs(wt%)	MMs(Dismeter/nm)
$P(AM_{25}/HMA_0)$-$MMs_{(1.0,349)}$	25	0	1.0	349
$P(AM_{25}/HMA_2)$-$MMs_{(0,0)}$	25	2	0	0
$P(AM_{25}/HMA_2)$-$MMs_{(0.5,349)}$	25	2	0.5	349
$P(AM_{25}/HMA_2)$-$MMs_{(1.0,349)}$	25	2	1.0	349
$P(AM_{25}/HMA_2)$-$MMs_{(1.5,349)}$	25	2	1.5	349
$P(AM_{25}/HMA_2)$-$MMs_{(1.0,103)}$	25	2	1.0	103
$P(AM_{25}/HMA_2)$-$MMs_{(1.0,214)}$	25	2	1.0	214
$P(AM_{25}/HMA_2)$-$MMs_{(1.0,300)}$	25	2	1.0	300
$P(AM_{25}/HMA_2)$-$MMs_{(1.0,424)}$	25	2	1.0	424

FTIR detection

The chemical structure of MMs was detected by a Nicolet iS-50 FTIR spectrometer using 64 scans at a resolution of 4 cm-1. Before measurement, the latex containing MMs would be freeze-dried in a freeze vacuum drier (FDU-2110, EYELA).

DLS measurement

The particle size and particle size distribution of MMs were characterized with American Brookhaven 90Plus Particle Size Analyzer. The laser light-scattering measurements were set as 90°. The samples of MMs were diluted with deionized water to 1/1000 of the original concentration for analysis. Five tests were measured for each sample. Then the average particle size and the size distribution were obtained.

Particle morphology

The particle morphology and distribution could be observed by transmission electron microscopy (TEM) (JEOL 1210,Japan). The accelerating voltage was set at 100 kv. Samples were prepared as follows. The latex was diluted with Deionized water to an appropriate concentration (about 0.1 mg/mL) and dropped onto the copper wire mesh. Magnification photograph was 50000 times the scale was 500nm in picture.

Mechanical property

The tensile tests of the hydrogels were carried out by a tensile tester (SHIMADZU, model AGS-X, 100N, Japan) at room temperature. The samples were cut into a dumbbell shape (length 30mm, gauge length 12 mm, width 4 mm, thickness 3 mm). The dumbbell-shaped samples were clamped and stretched at a constant velocity of 40 mm/min. The fracture stress σf and fracture strain εf were measured from tensile curves. For hysteresis measurement, the samples were first stretched to a maximum extension ratio λ = 15 and then unloaded. The dissipated energy (Uhys) was estimated by area below the stress–strain curves or between the loading–unloading curves. Tearing testing was performed using commercial tensile tester(SHIMADZU, model AGS-X, 100N, Japan). The gel samples were cut into a trousers shape (40 mm in length, 12 mm in width, and 3 mm in thickness) WITH AN initial notch of 20 mm. The two arms of the samples were clamped, in which the one arm was fixed, while the other one was pulled at 40 mm/min. The tearing energy (T) was estimated by[7]

$$T = \frac{2F_{ave}}{w}$$

Where F_{ave} was the average force of peak values during steady-state tear, and w was the thickness of the samples.

Rheological test

Dynamic rheological measurements were performed on a physical MCR 2000 rheometer (AR 2000ex). The dynamic viscoelastic properties (storage modulus G'and loss modulus G"of hydrogels were determined at different frequency of 0.01-100Hz. Frequency sweep tests for the samples were carried out at 25 °C using a parallel plate geometry (25mm diameter).

Morphology observation

The fracture section of hydrogels was observed by Scanning Electron Microscope (SEM) (JSM 6510). The samples were freeze-dried in a freeze vacuum drier (FDU-2110, EYELA) and immediately kept in liquid nitrogen for 3 minutes to break. All samples were sputtered with platinum before measurement and the magnification factor was 2000 or 5000 times.

Results and Discussion

Characterization of MMs crosslinked hydrogels

In our approach, the uniform-sized MMs were synthesized by using BA as a main component and BCPA as a crosslinker in an aqueous medium by a free radical polymerization, shown in Fig. 1(a). BA could be reacted with DCPA by using KPS as an initiator and MMs with a certain crosslinking degree were obtained. The aggregation and coalescence of MMs could be avoided due to the presence of SDS as an emulsifier. Moreover, the size of MMs could also be controlled by adding different quantity of emulsifiers and electrolytes (Na_2CO_3). DCPA with a Double-Loop structure could afford sufficient steric hindrance so that the unreacted carbon double bonds of DCPA would exist on the surface of MMs. As a result, MMs with pendent double bonds could synthesize with other vinyl monomers as chemical crosslinking agents. The chemical structure of MMs was characterized by FTIR spectroscopy and illustrated in Fig.2. It was found that the wavenumbers at 1654.2 and 1571.4(cm-1) showed characteristic peaks of pendent double bonds of DCPA in the FTIR patterns. The particle size and distribution of MMs were also obtained according to the particle size analyzer measurement and TEM, and illustrated in Fig.3. The mean diameters of MMs were 103 nm, 214 nm, 300 nm, 349 nm and 424 nm, respectively.

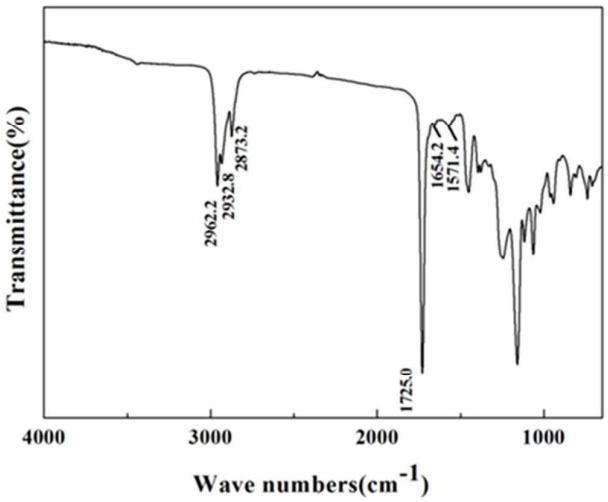

Fig. 2 FTIR spectrometer of MMs.

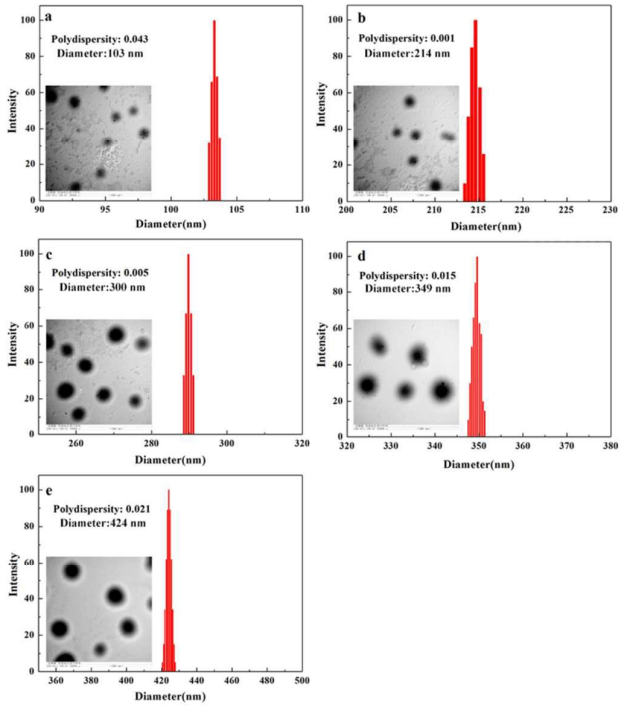

Fig. 3 Particle size and distribution of MMs by a size analyzer measurement and TEM.

The formation of MMs crosslinked hydrogels was carried out by a radical polymerization, meaning that monomers would form growing chains after initiation. If the growing chains encountered residual carbon double bonds of MMs, the hydrogels would be prepared using MMs as chemical crosslinkers. Meanwhile, the hydrophobic side chains from HMA would be self-assembled into physical crosslinked micelles. Moreover, if the hydrophobic side chains encountered hydrophobic components of MMs, the physically crosslinking centers would also be formed in the hydrogels. Therefore, MMs would become chemical crosslinkers and form partly hydrophobic associated points with hydrophobic components from HMA due to their intermolecular interaction. Based on this hypothesis, a schematic structure of MMs crosslinked hydrogels was shown in Fig. 1(b).

Mechanical Properties of Hydrogel

The high toughness of MMs crosslinked P(AM/HMA) hydrogels was demonstrated through stabbing, knotted stretching, loading and compressing experiments. Fig.4(a) showed puncture resistant properties of hydrogels and the results indicated that there was no damage or penetration for sheet-shaped hydrogels. Subsequently, the knotted stretching experiment of cylinder-shaped hydrogels was shown in Fig.4(b) and indicated highly stretching property (10 times its original length) without any fracture. Moreover, Fig.4(c) showed the loading experiment of cylinder-shaped hydrogels and 350g of hollow iron pipe could be easily lifted. Also, the compression of hydrogels was exhibited, as shown in Fig.4(d), and it was found that the hydrogels could still recover its original dimension after unloading. All experiments confirmed elasticity and toughness and puncture resistant properties of P(AM/HMA)-MMs hydrogels.

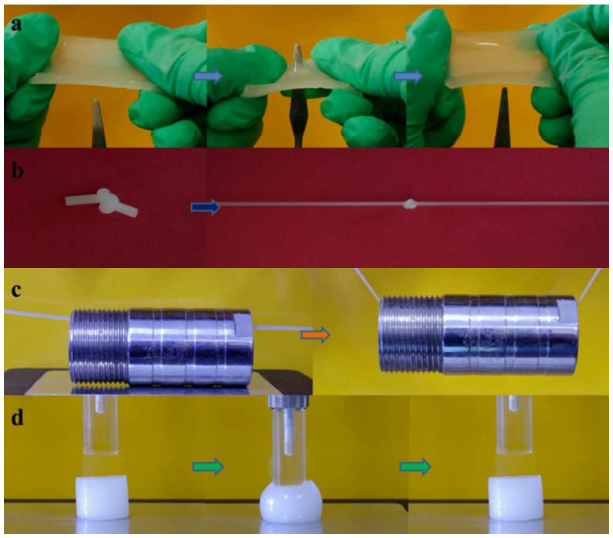

Fig. 4 High toughness of MMs crosslinked P(AM/HMA) hydrogels through a) stabbing, b) knotted stretching, c) loading and d) compressing experiments (MMs content was 1.0wt% in adding monomers and the diameter was 349 nm in adding monomers).

Subsequently, We compared tensile properties among PAM-MMs, P(AM/HMA), P(AM/HMA/PEGAA) and P(AM/HMA)-MMs hydrogels. As shown in Fig. 5a, PAM-MMs hydrogels with a chemically crosslinking network exhibited poor extensibility and strength. The fracture stress σ_f and fracture strain ε_f were 0.035 MPa and 552 %, respectively. In contrast, P(AM/HMA) hydrogels with a single hydrophobic associated network exhibited longer elongation of break and higher mechanical strength. The fracture stress σ_f and fracture strain ε_f were 0.207 MPa and 3233 %, respectively, P(AM/HMA/PEGAA) hydrogels with hydrophobic associated network and chemically crosslinking network also exhibited higher mechanical property. The fracture stress σ_f and fracture

strain ε_f were 0.367 MPa and 4285 %, respectively. However, It was obviously demonstrated that the mechanical properties of P(AM/HMA)-MMs hydrogels were significantly enhanced by adding with a small amount of MMs (1.0wt% for AM and HMA). The fracture stress σ_f and fracture strain ε_f were 0.555 MPa and 5533%, respectively. That means that MMs could not only become a chemical crosslinker but also play a synergistically hydrophobic crosslinking center in hydrogels. We investigated tearing mechanical properties of P(AM/HMA), P(AM/HMA/PEGAA) and P(AM/HMA)-MMs hydrogels. Fig.5b showed that the tearing energy of P(AM/HMA)-MMs hydrogels was about 800Jm^{-2}, Much higher than that of P(AM/HMA) hydrogels (about 350Jm^{-2}) and P(AM/HMA/PEGAA) hydrogels (about 550Jm^{-2}). This also indicated that MMs could enhance the fracture propagation and puncture resistance of hydrogels. The hydrophobic side chains of HMA would be entangled with hydrophobic components of MMs to form a micellar structure. The physically crosslinking centers with curl hydrophobic chains would slide, stretch and dissipate a large amount of energy when the hydrogels were loaded and deformed. Compared the stress–strain curves of the three types of hydrogels during a loading–unloading cycle to reveal their energy dissipation capacity, the sliding of chain could dissipate energies. As shown in Fig.5c, at λ = 15, dissipated energies of P(AM/HMA)-MMs hydrogels (350KJm^3) were much higher than P(AM/HMA) hydrogels (223KJm^3) and P(AM/HMA/PEGAA) hydrogels (230KJm^3). The physically crosslinking centers with curl hydrophobic chains would slide during the deformation. Therefore, MMs crosslinked P(AM/HMA) hydrogels exhibited a very excellent mechanical property.

Then, the effect of the MMs content on the mechanical properties of P(AM/HMA)-MMs hydrogels was measured and shown in Fig. 6. With the increase of MMs contents from 0wt% to 1.5wt%, the tensile stress of hydrogels would constantly increase and then decrease. The maximum yield stress of P(AM/HMA)-MMs hydrogels (1.0wt% of MMs for AM and HMA) achieved 0.55MPa. Moreover, the fracture elongation of hydrogels (1.0wt%-1.5wt% of MMs for AM and HMA) exhibited more than 55 times its original length. It was due to chemical crosslink and hydrophobic molecular slippage of MMs in hydrogels. One interesting phenomenon was observed that an obvious buffering platform existed in the tensile curve for P(AM/HMA)-MMs hydrogels (1.0wt%-1.5wt% of MMs for AM and HMA) when the stress reached critical yield stress. The stress was almost unchanged in the buffering zone with the increase of strain. When the stress was close to the yield stress, MMs could produce enormously elastic deformation due to the performance of rubber particles themselves. Therefore, MMs embedded in hydrogels would play multiple roles of chemically crosslinking, physically hydrophobic entanglement and rubber-like toughening zones.

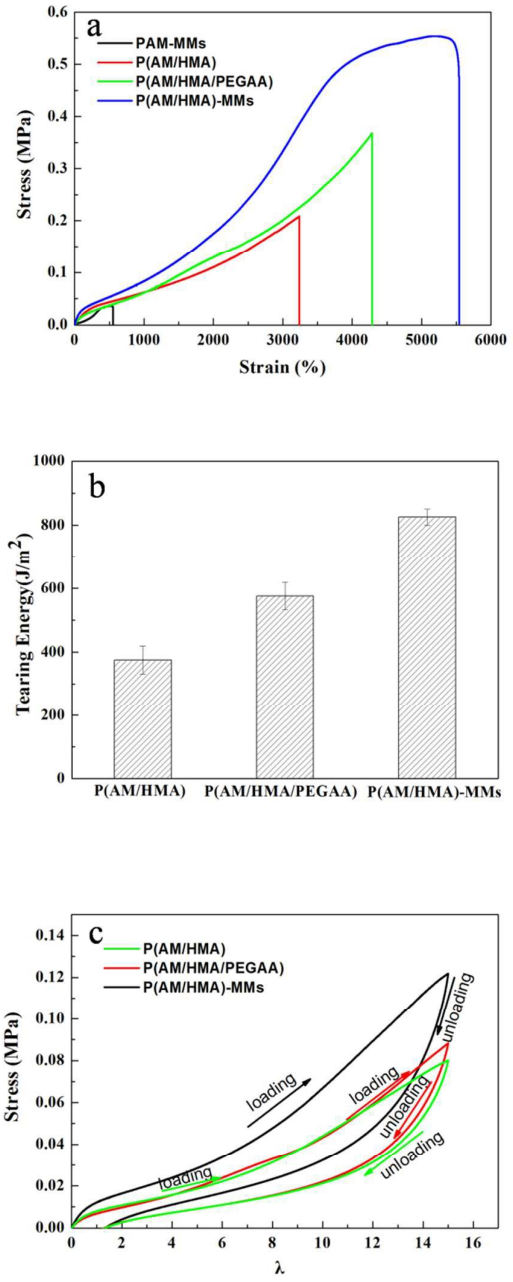

Fig.5 a) Tensile curves of PAM-MMs, P(AM/HMA), P(AM/HMA/PEGAA) and P(AM/HMA)-MMs hydrogels. b) Tearing energies of P(AM/HMA), P(AM/HMA/PEGAA) and P(AM/HMA)-MMs hydrogels. C) The first cyclic loading–unloading stress–strain curves of P(AM/HMA), P(AM/HMA/PEGAA) and P(AM/HMA)-MMs hydrogels. (MMs content was 1.0wt% for AM and HMA, and the diameter was 349 nm in adding monomers).

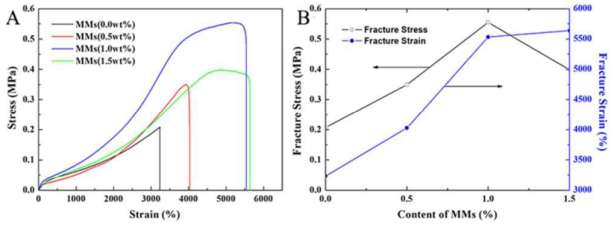

Fig. 6 Tensile curves of P(AM/HMA)-MMs hydrogels with different MMs contents (MMs diameter was 349 nm in adding monomers)

The particle size of MMs had also an important effect on the mechanical properties of the hydrogels and the tensile properties were shown in Fig. 7. The fracture stress of hydrogels showed lightly a trend of first increase and then decrease with the increase of particle size of MMs in Fig. 7a. The maximum stress was 0.55 MPa for P(AM/HMA)-MMs with a 349 nm of MMs. It was meaning that at the same content of MMs the mechanical properties were determined by the effectiveness of each crosslinker and crosslinker number. The effectiveness of each crosslinker was proportional to the particle size, and crosslinker number was inversely proportional to the particle size. The combined effect showed a trend of first increase and then decrease with the increase of particle size of MMs, The optimum value of the combined effect appeared in the particle size of 349nm. Moreover, the fracture strain exhibited a similar trend for P(AM/HMA)-MMs with different particle sizes of MMs in Fig. 7b.

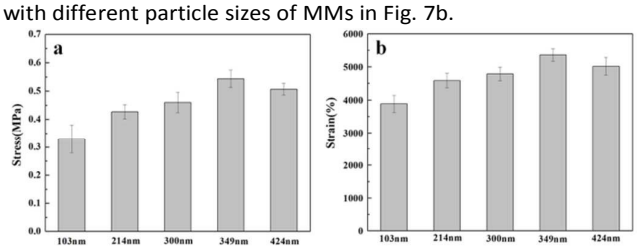

Fig. 7 Fracture stress and fracture strain of P(AM/HMA)-MMs hydrogels with different particle size of MMs (MMs content was 1.0wt% for AM and HMA in adding monomers)

Rheology Properties of Hydrogels

In order to reveal the relationship between microstructure and macroscopic mechanical properties, the effect of the MMs content on the rheological properties of the hydrogels was investigated[31]. As shown in Fig.8, it was clear that introducing MMs had an obvious effect on storage modulus (G′) and loss modulus (G″), and all samples were dominated elastic materials because of G′ exceeding G″ in the measuring frequency range. With the increase of MMs content, storage modulus (G′) decreased, demonstrating that the hydrogels became more flexible because of leak interaction of hydrophobic MMs and hydrophilic matrix. Otherwise, loss modulus (G″) increased, indicating that the number of instable or reversible crosslinking points increased. The crosslinking points were easily destructed under the outside force, leading to move of molecular chains and produce viscous deformation. As a result, hydrogels exhibited high fracture strain in the tensile test. The result was consistent with that in Fig.6 and also indicated that the fracture strain of the hydrogel could be easily enhanced by introducing MMs. Moreover, the ratio of G″ / G′ (tan δ) indicated the viscosity of the material[32]. As shown in Fig 9, the ratio of tan δ also increased with the increase of content of MMs due to increasing instable or reversible crosslinking points.

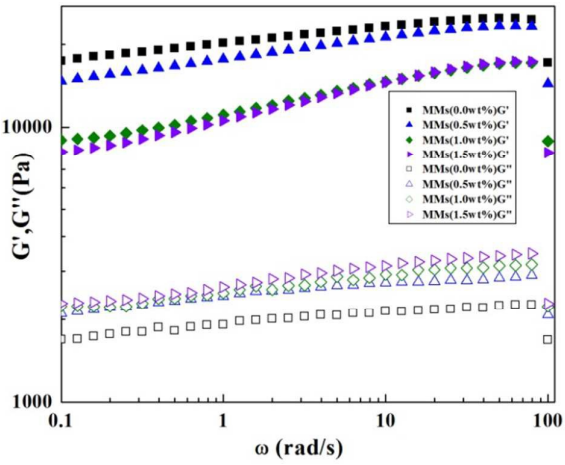

Fig. 8 Storage modulus (G') and loss modulus (G″) of P(AM/HMA)-MMs hydrogels at different frequencies(mean diameters of MMs were 349 nm in adding monomers)

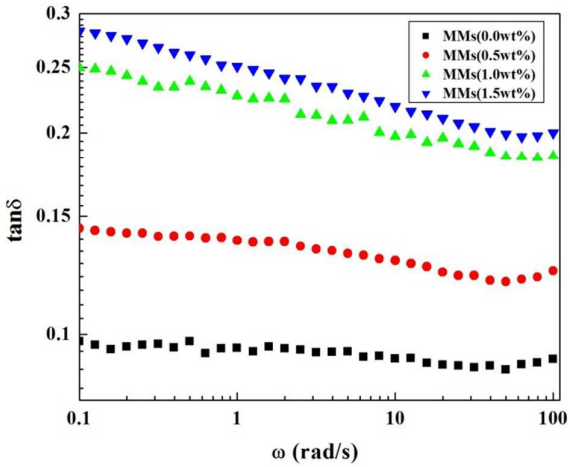

Fig. 9 Ratio of loss modulus (G″) to storage modulus (G') of P(AM/HMA)-MMs hydrogels at different frequencies(mean diameters of MMs were 349 nm in adding monomers)

Observation of morphology

To confirm the microstructure of MMs in P(AM/HMA) hydrogels, SEM was employed to observe the surface of brittle failure for P(AM/HMA)-MMs hydrogels and the image was shown in Fig. 10. It was clearly shown that MMs could be embedded in P(AM/HMA)-MMs hydrogels matrix, indicating that the forces between MMs and matrix was very strong. MMs as chemical crosslinkers and hydrophobic associated centers could be dispersed so uniformly in hydrogels matrix that the homogeneous network structure could be formed in hydrogels. Moreover, MMs themselves could produce enormously elastic deformation under the forces. As a result,

P(AM/HMA)-MMs hydrogels exhibited excellent mechanical properties in the tensile test.

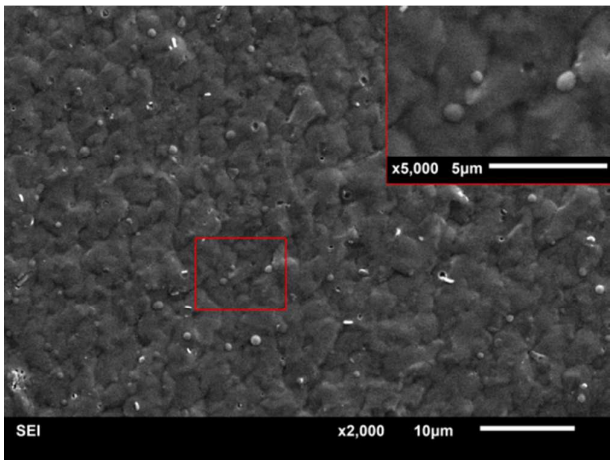

Fig.10 Microscopic SEM image of MMs crosslinked P(AM/HMA) hydrogels (MMs content was 1.0wt% in adding monomers and the diameter was 349 nm in adding monomers).

Conclusions

In summary, highly tough and puncture resistant P(AM/HMA)-MMs hydrogels were successfully prepared by the introduction of macromolecular microspheres as chemical and physical crosslinking centers. The MMs crosslinked hydrogels exhibited an extraordinary tensile strength and elongation at break comparing to traditional hydrogels toughened by simple hydrophobic segments. Moreover, MMs could produce enormously elastic deformation themselves due to the nature of rubber particles, leading to long fracture elongation of over 55 times their original length. Also, the P(AM/HMA)-MMs hydrogels exhibited an excellent puncture resistant property. Therefore, the novel strategy, inspired by toughening mechanism of rubber-enhanced plastics, had proved to be effective in toughening hydrogels and would open a new avenue for extensive biomedical applications of tough hydrogels, such as artificial tendon, cartilage, skins and so on.

Acknowledgements

This research was supported by a grant from National Natural Science Foundation of China (NSFC) (Nos. 51473023 and 51103014).

References

1 S. H. M. Söntjens, D. L. Nettles, M. A. Carnahan, L. A. Setton,M. W. Grinstaff, Biomacromolecules, 2005, **7,** 310.
2 K. Y. Lee, D. J. Mooney, Chem. Rev., 2001, **101**, 1869.
3 N. Huebsch, C. J. Kearney, X. Zhao, J. Kim, C. A. Cezar, Z. Suo, D. J. Mooney, Proc. Natl. Acad. Sci. U.S.A., 2014, **111**, 9762.
4 A. Servant, V. Leon, D. Jasim, L. Methven, P. Limousin, E. V. Fernandez-Pacheco, M. Prato, K. Kostarelos, Adv. Healthcare Mater., 2014, **3**, 1334.
5 A. S. Hoffman, Adv. Drug Deliv. Rev., 2002, 54, 3.
6 G. D. Nicodemus, S. J. Bryant, Tissue Eng. Part B Rev., 2008, **14**, 149.
7 Q. Chen, L. Zhu, H. Chen, H. L. Yan, L. N. Huang, J. Yang, J. Zheng, Adv. Funct. Mater., 2015, **25**, 1598.
8 J. P. Gong, Y. Katsuyama, T. Kurokawa, Y. Osada, Adv. Mater., 2003, **15**, 1155.
9 Y. Okumura, K. Ito, Adv. Mater., 2001, **13**, 485.
10 K. Haraguchi, T. Takehisa, Adv. Mater., 2002, **14**, 1120.
11 K. Haraguchi, H. J. Li, Angew. Chem. Int. Ed., 2005, **44**, 6500.
12 K. Haraguchi, H. J. Li, Macromolecules, 2006, **39**, 1898.
13 M. K. Shin, G. M. Spinks, S. R. Shin, S. I. Kim, S. J. Kim. Adv. Mater., 2009, **21**, 1712.
14 T. Sakai, T. Matsunaga, Y. Yamamoto, C. Ito, R. Yoshida, S. Suzuki, N. Sasaki, M. Shibayama, Macromolecules, 2008, **41**, 5379.
15 Q. Wang, J. Mynar, M. Yoshida, E. Lee, M. Lee, K. Okuro, K. Kinbara, T. Aida, Nature, 2010, **463**, 339.
16 T. Huang, H. G. Xu, K. X. Jiao, L. P. Zhu, H. R. Brown, H. L. Wang, Adv. Mater., 2007, **19**, 1622.
17 T. Huang, H. G. Xu, K. X. Jiao, L. P. Zhu, H. R. Brown, H. L. Wang, Adv. Mater., 2007, **19**, 1622.
18 C. C. He, K. X. Jiao, X. Zhang, M. Xiang, Z. Y. Li, H. L. Wang, Soft Matter, 2011, **7**, 2943.
19 G. Q. Jiang, C. Liu, X. L. Liu, Q. R. Chen, G. H. Zhang, M. Yang, F. Q. Liu, Polymer, 2010, **51**, 1507.
20 G. Q. Jiang, C. Liu, X. L. Liu, G. H. Zhang, M. Yang, Q. R. Chen, F. Q. Liu, J. Macromol. Sci. Part A: Pure Appl. Chem., 2010, **47**, 335.
21 G. Q. Jiang, C. Liu, X. L. Liu, G. H. Zhang, M. Yang, F. Q. Liu, Macromol. Mater. Eng., 2009, **294**, 815.
22 M. Yang, C. Liu, Z. Y. Li, G. Gao, F. Q. Liu, Macromolecules, 2010, **43**, 10645.
23 M. Saric, H. Dietsch, P. Schurtenberger, Colloids Surf. A, 2006, **291**, 110.
24 T. Cai, G. N. Wang, S. Thompson, M. Marquez, Z. B. Hu, Macromolecules, 2008, 41, 9508.
25 K. Haraguchi, T. Takehisa, Adv. Mater., 2002, 14, 1120.
26 K. Haraguchi, H. J. Li, Angew. Chem. Int. Ed., 2005, 44, 6500.
27 B. J. Liu, M. Y. Zhang, C. Zhou, L. Ren, H. L. Cheng, Y. H. Ao, H. X. Zhang, Colloid. Polym. Sci., 2013, **291**,2385.
28 B. J. Liu, M. Y. Zhang, H. L. Cheng, Z. Y. Fu, T. T. Zhou, H. Chi, H. X. Zhang, Colloid. Polym. Sci., 2014, **292,** 519.
29 E. H. Merz, G. C. Claver, M. Baer, J. Polym. Sci., 1956, **22,** 325.
30 C. B. Bucknall, R. R. Smith, polymer, 1965, **6**, 437.
31 M. J. D. Nugent, A. Hanley, P. T. Tomkins, C. L. Higginbotham, J. Mater. Sci. Mater. Med., 2005, **16**, 1149.
32 J. Y. Sun, X. H. Zhao, W. R. K. Illeperuma, O. Chaudhuri, K. H. Oh, D. J. Mooney, J. J. Vlassak, Z. G. Suo, Nature, 2012, **498**, 133.